Performance Evaluation of CE-OFDM in PLC Channel

El Ghzaoui Mohammed elghzaoui.mohammed@gmail.com
Laboratory of Transmission and Data processing, University Sidi Mohammed Ben Abdellah, Fez,

Belkadid Jamal belkadid@gmail.com
Laboratory of Transmission and Data processing, University Sidi Mohammed Ben Abdellah, Fez,

Benbassou Ali alibenbassou@gmail.com
Laboratory of Transmission and Data processing, University sidi Mohammed ben Abdellah, Fez,

Abstract

One major drawback associated with an OFDM system is that the transmitter's output signal may have a high peak-to-average ratio (PAPR). High levels of PAR may be a limiting factor for power line communication (PLC) where regulatory bodies have fixed the maximum amount of transmit power. To overcome this problem, many approaches have been presented in the literature. One potential solution for reducing the peak-to-average power ratio (PAPR) in an OFDM system is to utilize a constant envelope OFDM (CE-OFDM) system. This paper describes a CE-OFDM based modem for Power Line Communications (PLC) over the low voltage distribution network. The impact of the electrical appliances on the signal transmission is investigated. The good performances of the BER have been checked by the simulation platform of real PLC channel using Matlab. Finally, CE-OFDM-CPM is compared with conventional OFDM under HomePlug AV..

Keywords: OFDM, CE-OFDM, CPM, BER, PAPR

1. INTRODUCTION

In home networks advanced communication technologies has allowed the Power Line Communication (PLC) channel to be a transmission medium that enables the transferring of high-speed digital data over the classical indoor electrical wires. Power Line Communications [1, 2, 3] have been the subject of an important research work. At the same time, the growing demand for multimedia communications provides a good prospect for PLC as a promising transmission technique for the “last mile” access network. However, the main characteristics of the power line channel seem quite unfavorable: multipath reflections induced by impedance mismatches, changes in the channel transfer function [4] due to the switching of electrical devices, a highly diverse noise environment, and so forth. Therefore, an efficient transmission scheme has to include robust techniques in order to face the difficulties of such a medium and to get reliable and

spectrally efficient transmissions. In this study, we investigate the influences of some switching power devices on PLC adapters.
Orthogonal frequency division multiplexing (OFDM) [5, 6, 7] modulation using orthogonal subcarriers reduces the delay spread by increasing robustness to multipath fading and can use overlapped bandwidth due to orthogonality on frequency domain. Thus, OFDM has been adopted for high speed data transmission of multimedia traffic such as HomePlug A/V and Mobile WiMax. However, OFDM also has a drawback of a high PAPR (peak-to-average-power-ratio). This high PAPR takes place due to parallel processing of a number of data at once using a fast Fourier transform (FFT) processor. Implementation of multicarrier system needs more precision Digital-to-Analog Converter (DAC) in Transmitter and more precision Analog-to-Digital Converter (ADC) in Receiver. The DAC clips all samples that exceed certain maximum amplitude, the clip level. Setting this level is a compromise between clipping probability and quantization noise level: decreasing the chip level will increase the average clip noise but decrease the quantization noise. It is usually set to that the total Signal-to-Noise Ratio (SNR) is minimized. A lower PAR will increase the SNR or allow for a DAC with lower resolution to be used. In the literature, many PAR reduction schemes have been studied, such as block coding [8], clipping [9], trellis shaping [10] and selected mapping (SLM) [11].
To alleviate this problem, constant envelope OFDM (CE-OFDM) signal has been introduced in [12, 13, 14], which combines orthogonal frequency division multiplexing and phase modulation or frequency modulation. Furthermore, by utilizing continuous phase modulation (CPM) in a CE-OFDM system, the PAPR can be effectively reduced to 0 dB. Although the CPM has low spectral efficiency, it features low system complexity and favorable performance due to low PAR and robustness to amplitude variation and impulsive noise [15]. The CPM decreases the side lobe of the power spectrum by means of continuously connecting the phase that contains the information.
This paper is organized as follows. Next section describes the PAPR of OFDM system. In section 3, we give a brief insight on CPM modulation. Then the CE-OFDM-CPM signal is introduced in section 4. Experimental and Simulation results are presented in Section 5 and Section 6 concludes the paper.

2. PAPR OF OFDM SYSTEM

The OFDM baseband waveform can be represented by

$$m(t) = \sum_{k=0}^{N-1} I_k e^{j2\pi \frac{k}{T_B} t} \qquad 0 \le t \le T_B \qquad (1)$$

N is the number of subcarriers, T_B is the signaling interval, and data symbol I_k modulates the k[th] subcarrier $e^{j\pi \frac{k}{T_B} t}$. The data symbols are chosen from a complex set defined by an M-point signal constellation such as PSK or QAM. Consider sampling $m(t)$ without cyclic prefix, at the sampling rate $f_{sa} = \frac{JN}{T_B}$ samp/s, where $J \ge 1$ is the oversampling factor. The signal samples are:

$$m[n] = \sum_{k=0}^{N-1} I_k e^{j2\pi \frac{k}{N_B J} n} \qquad n = \{0,1,........., N_B - 1\} \qquad (2)$$

It can be seen that the sequence $\{m[n]\}$ can be interpreted as the inverse discrete Fourier transform (IDFT) of the OFDM data block *I* with $(J-1)N$ zero padding. It is well known that PAPR of the continuous-time OFDM signal cannot be obtained precisely by the use of Nyquist rate sampling, which corresponds to the case of $J = 1$. It is shown in [16] that $J = 4$ can provide sufficiently accurate PAPR results. The PAPR computed from the J-times oversampled time-domain signal samples is given by

$$PAPR_s = \frac{\max_{0 \le n \le JN} |m(n)|^2}{E_s\{|m[n]|^2\}} \qquad (3)$$

Where E{.} denotes expectation.
The instantaneous signal power, $|s(t)|^2 = \Re^2\{s(t)\} + \Im^2\{s(t)\}$, with the peak and average signal power, are plotted in Figure 1. For this example the peak-to-average power ration is more than 7.9 dB.
There have been many schemes proposed in the research literature aimed at reducing the impact of the PAPR problem. All PAPR reduction techniques have some advantages and disadvantages. These PAPR reduction techniques should be chosen carefully for getting the desirable minimum PAPR. In the following section we introduce an improved PAPR reduction scheme using constant envelope modulation.

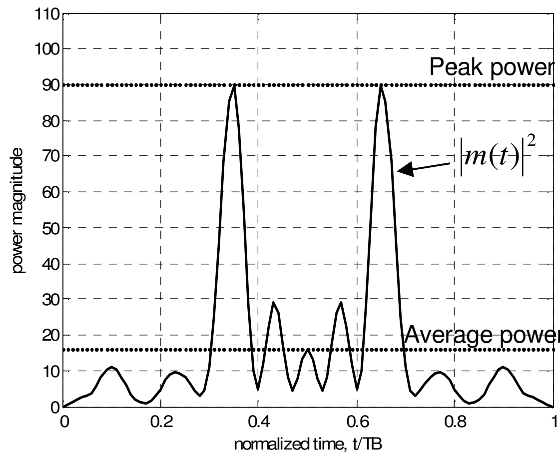

FIGURE 1: Instantaneous signal power of OFDM signal, also showing average and peak powers. N=16, $I_k \in \{\pm 1\}$

3. CONTINUOUS PHASE MODULATION

Continuous phase modulation (CPM) is a good example of nonlinear modulation with memory. Signal dependence is introduced purposely to shape the spectrum of the transmitted signal to achieve better spectral efficiency. As a result, CPM modulation is a nonlinear modulation scheme with memory [17]. Furthermore, CPM is typically implemented as a constant-envelope waveform.
The CPM baseband signal is given by:

$$x(t) = Ae^{j\phi(t,I)} \qquad (4)$$

where A is the signal energy and the phase is given by

$$\phi(t,I) = \phi_0 + 2\pi \sum_{k=-\infty}^{n} h_k I_k q_k(t - kT), \quad nT \le t < (n+1)T \qquad (5)$$

where ϕ_0 is the phase memory, I_k is the sequence of M-ary information symbols, h_k is a sequence of modulation indices and the waveform *q*(t) can be represented as,

$$q(t) = \int_0^t g(\tau)d\tau \qquad (6)$$

Normally, the function *g*(t) is a smooth pulse shape over a finite time interval *0 ≤ t ≤ LT* and zero outside. Thus, L is the pulse length and T is the symbol period. From the definition of the above class of constant amplitude modulation schemes the pulse *g*(t) is defined in instantaneous frequency and its integral *q*(t) is the phase response [18].

4. CE-OFDM-CPM SIGNAL DESCRIPTION

4.1. CE-OFDM Signal Définition

Consider the baseband OFDM waveform:

$$m(t) = \sum_{i}\sum_{k=1}^{N} I_{i,k} q_k(t - iT_B) \quad (7)$$

Where $\{I_{i,k}\}$ are the data symbols and $\{q_k(t)\}$ are the orthogonal subcarriers. For conventional OFDM the baseband signal is up-converted to band-pass as:

$$\begin{aligned} y(t) &= \Re\{m(t)e^{j2\pi f_c t}\} \\ &= A_m(t)\cos[2\pi f_c t + \phi_m(t)] \end{aligned} \quad (8)$$

f_c : Carrier frequency

Where $A_m(t) = |m(t)|$ and $\phi_m(t) = \arg[m(t)]$. For real-valued $m(t)$, $\phi_m(t) = 0$ and $y(t)$ is simply an amplitude modulated signal. For CE-OFDM, $m(t)$ is passed through a phase modulator prior to up-conversion. The baseband signal is $s(t) = Ae^{j\alpha m(t)}$ where α is a constant. The band-pass signal For real-valued *m*(t) is ,

$$y(t) = \cos[2\pi f_c t + \alpha m(t)] \quad (9)$$

Therefore $y(t)$ is a phase modulated signal.

The OFDM signal is phase modulated onto a carrier signal to obtain a constant envelope signal with 0dB PAPR. CE-OFDM requires a real-valued OFDM [19] message signal, that is, $\phi_m(t) = 0$. Therefore the data symbols in (7) are real-valued, this one dimensional constellation is known as pulse-amplitude modulation (PAM). Thus the data symbols are selected from an M-PAM set. The subcarriers $q_k(t)$ must also be real-valued, and may be expressed as:

$$q(t) = \begin{cases} \cos(2\pi kt/T_B) & 0 \le t < T_B \quad k < N, \\ \sin(2\pi(k - N/2)t/T_B) & 0 \le t < T_B, \quad k > N/2 \\ 0 & \text{otherwise.} \end{cases} \quad (10)$$

For k = 1, 2, . . . , N,

The subcarrier orthogonality condition holds:

$$\int_{iT_B}^{(i+1)T_B} q_{k1}(t - iT_B)\, q_{k2}(t - iT_B)\, dt = \begin{cases} E_q & k_1 = k_2 \\ 0 & k_1 \ne k_2 \end{cases} \quad (11)$$

Where $E_q = T_B / 2$

The baseband CE-OFDM signal is,

$$s(t) = Ae^{j\phi(t)} \quad (12)$$

Where A is the signal amplitude.

The phase signal during the i^{th} block is written as:

$$\phi(t) = \theta_i + 2\pi h c_N \sum_{k=1}^{N} I_{i,k} q_k(t - iT_B), \quad iT_B \le t < (i+1)T_B \quad (13)$$

Where

$$\theta(t) = \phi(iT - \varepsilon) - \phi(iT + \varepsilon), \quad \varepsilon \to 0$$

The phase memory θ_i may be used in conjunction with a phase unwrapper at the receiver to ensure a continuous phase at the symbol boundaries and hence better spectral containment [20, 12]. Here *h* refers to modulation index; N is the number of sub-carriers $I_{n,k}$ represents M-PAM data symbols; T_B is the i^{th} block interval, and $q_k(t)$ represents the set of subcarrier waveforms. The normalizing constant, c_N , is set to $c_N = \sqrt{\frac{2}{N\sigma_I^2}}$ where σ_I is the variance of the data symbols, and consequently the variance of the phase signal will be $\sigma_\phi^2 = (2\pi h)^2$. Assuming that the data is independent and identically distributed, it follows that $\sigma_I^2 = \frac{M^2-1}{3}$.

To guarantee continuous phase, the memory terms set to

$$\theta_i = K\sum_{l=0}^{\infty}\sum_{k=1}^{N}[I_{i-l,k}\, A_b(k) - I_{i-1-l,k}\, A_e(k) \qquad (14)$$

Where

$$K = 2\pi h c_N\ ,\ A_b(k) = q_k(0)\ ,\ A_e(k) = q_k(T_B - \varepsilon)\ ,\ \varepsilon \to 0\,.$$

The benefit of continuous phase CE-OFDM-CPM is a more compact signal Spectrum [20].

4.2. Spectral Efficiency

The effective double-sided bandwidth, defined as the twice the highest frequency subcarrier, of *m*(t) is:

$$W = 2\frac{N}{2T_B} = \frac{N}{T_B} \qquad (15)$$

The bandwidth of $s(t)$ is at least *W*, and depending on the modulation index the effective bandwidth can be greater than *W*. The RMS (root-mean-square) bandwidth is obtained by borrowing a result from analog angle modulation [21], [22],

$$B_{rms} = \sigma_\phi W = 2\pi h W \qquad (16)$$

As defined in (16), the RMS bandwidth can be less than *W*. A more suitable bandwidth is thus,

$$B_s = \max(2\pi h, 1)W \qquad (17)$$

The power density spectrum can be easily estimated by the Welch method [23] of periodogram averaging. Figure 2 shows Power Spectrum of CE-OFDM for different value of modulation index.

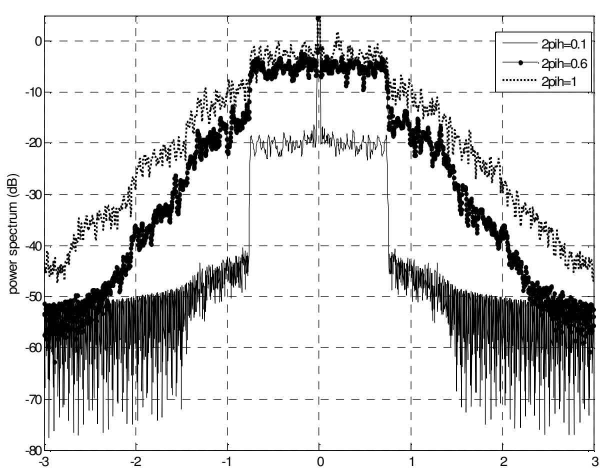

FIGURE 2: Power Spectrum of CE-OFDM-CPM. N=512

Since the modulation index controls the CE-OFDM spectral containment, smaller h can be used if a tighter spectrum is required. The tradeoff is that smaller h results in worse performance. Therefore, the system designer can trade performance for spectral containment, and visa versa, consequently the modulation index also controls the system performance. Figure 2 shows that the power spectrum of the CE-OFDM signal is nearly constant over the range $\left|\frac{f}{W}\right| < 0.8$. To calculate the spectral efficiency versus performance, the data rate must be defined, which for uncoded CE-OFDM is:

$$R = \frac{N \log_2(M)}{T_B} \qquad (18)$$

Using (17) as the effective signal bandwidth, the spectral efficiency is,

$$\eta = \frac{R}{B_s} = \frac{\log_2(M)}{\max(2\pi h, 1)} \quad b/s.Hz \qquad (19)$$

5. MEASUREMENTS AND SIMULATIONS RESULTS

We have made frequency response measurements for in-building power line channels in the frequency range of (1–100 MHz). As can be seen, the frequency response exhibits considerable frequency dependent variation, due to the specific wiring configurations encountered. The frequency dependent channel fading is the result of reflections and multipath propagation. One main source for reflection and multipath propagation is impedance discontinuity. There are many possible reasons for impedance discontinuity, such as change of gauge of wires connected to each other, connected loads or branch wires, etc.

5.1. Individual Appliances Connection

Electrical appliances connected or not connected to the network at anytime generate changes on network characteristics. We consider the topology in Figure 3. The electrical appliances at point B were varied as personal computer charger, cell phone charger, heater, and without electrical appliances. Figure 4, we plot the realization of a channel frequency response magnitude measured by network analyzer in downlink from a household for different electrical appliances. Measurements demonstrate that the impedance varies significantly from one electrical appliance to another.

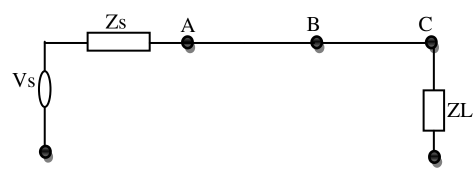

FIGURE 3: Power line network between sending and receiving ends.

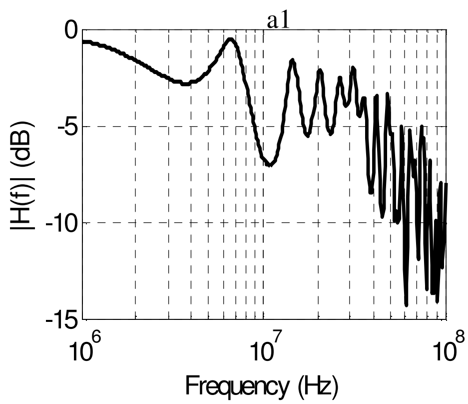

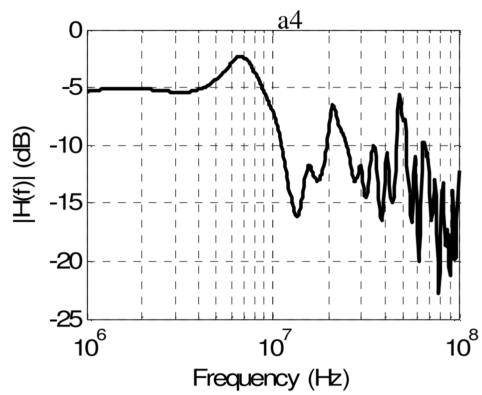

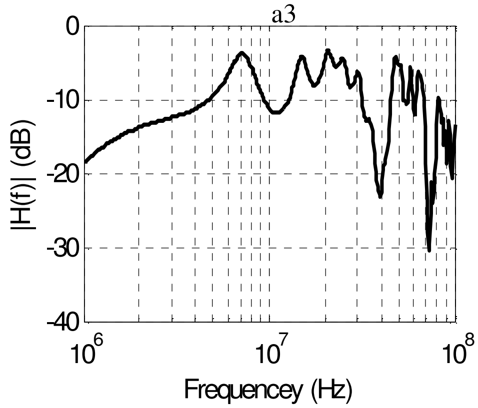

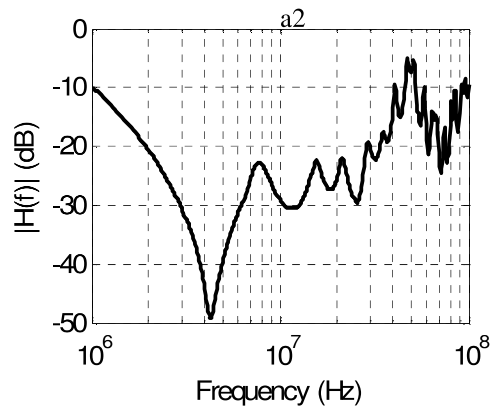

FIGURE 4: Experimental measurements of frequency response magnitude for different Electrical appliances (a1) without Electrical appliances (a2) heater, (a3) personal computer charger, (a4) cell phone charger.

5.2. Combinations of Appliance Connection

In Figure 5 the measurements results regarding the simultaneous connection of two outlet cable with a length of 1.5m, heater, personal computer charger, cell phone charger and arbitrary generator are recorded.

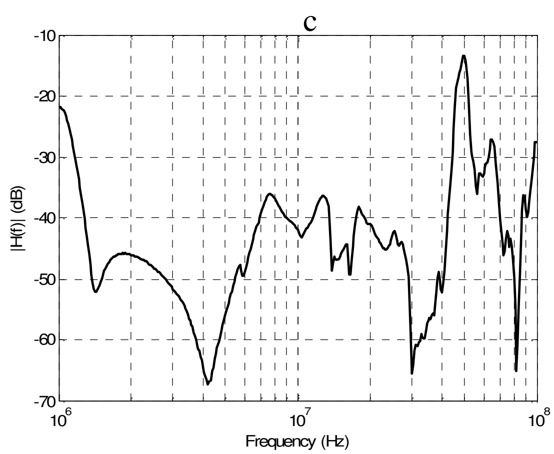

FIGURE 5: Experimental measurements of frequency response magnitude of arbitrary combinations of appliance connection.

5.3. NUMERICAL RESULTS

In this section, the bit error rate (BER) performance of the proposed CE-OFDM-CPM PLC system is investigated. The signal-to-noise ratio (SNR) is defined as E_b/N_0, where E_b is the received energy per information bit and N_0 is the power spectral density of the noise. The BER performance of CE-OFDM-CPM over PLC channel is evaluated using computer simulation. First let us see the influence of different electrical appliances on transition on PLC channel.

Figure 6 shows the performance of the CE-OFDM-CPM system for different electrical appliances cases. A good channel performance is seen for without electrical appliances with the bit error probability of 3.10^{-7} at a E_b/N_0 per bit of 20 dB. The power is 26 dB, 28 dB and 39 dB, for heater, personal computer charger, and cell phone charger, respectively. When the cell phone is connected the power loss is 39 dB indicating degraded performance. The results in Figure 6 show the dramatic performance degradation as a consequence of the severe frequency selectivity. The analysis of the results leads to a classification of the electrical appliances, according to their influence on the transmitted PLC signal in the narrow-band frequency range. Appliances such as cell phone charger cause a severe attenuation on the transmitted signal. For

example, Lin et al. showed that cell phone chargers caused serious degradation of the bandwidth of the PLC adapters [24]. The severe attenuation is related to the presence of the compensation capacitors of the devices. The signal levels are also affected by the transmitter and the distance of the connection point from the transmitter.
Figure 7 shows the performance of the CE-OFDM-CPM system for channel (c) (Combinations of appliances connection). A good channel performance is seen for without electrical appliances with the bit error probability of 10^{-7} at a E_b/N_0 per bit of 20 dB, but if the simultaneous connection of electrical appliances the power loss is 59 dB indicating degraded performance (the performance is severely degraded due to the several frequency selectivity).

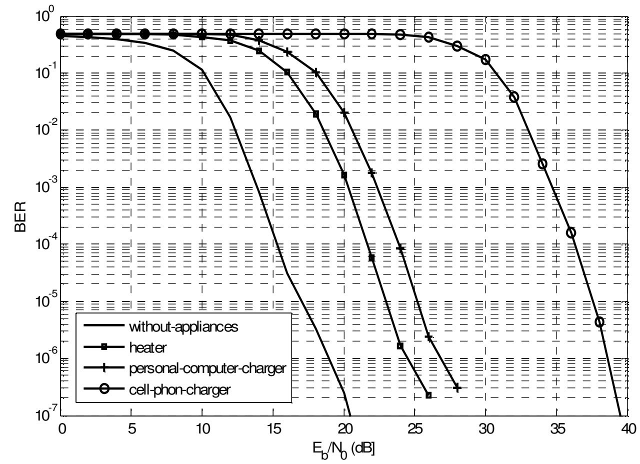

FIGURE 6: Performance of CE-OFDM in PLC channel for different Electrical appliances, (M=4, N=512, 2πh=1, J=4, MMSE).

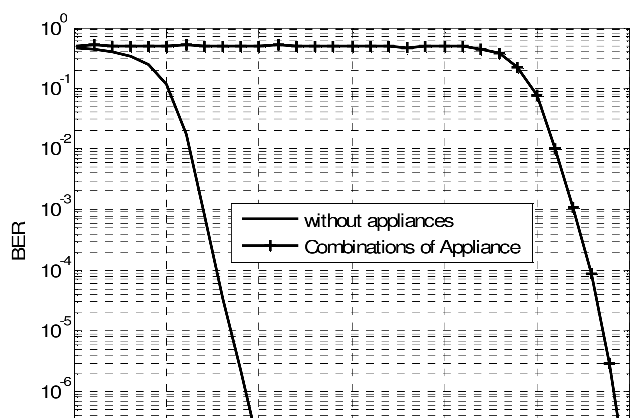

FIGURE 7: Performance of CE-OFDM in PLC channel for simultaneous connection of electrical appliances. (M=4, N=512, 2πh=1, J=4, MMSE).

In figure 8, the BER performances of CE-OFDM-CPM have been simulated and compared with OFDM system under *HomePlug AV*. In this case 2πh=0.8 and M=16. CE-OFDM-CPM is shown to outperform OFDM at high bit energy-to-noise. CE-OFDM-CPM is shown to outperform OFDM at high E_b/N_0. Alternatively, if operation at low E_b/N_0 is important, then CE-OFDM-CPM may not be well suited due to the threshold effect.

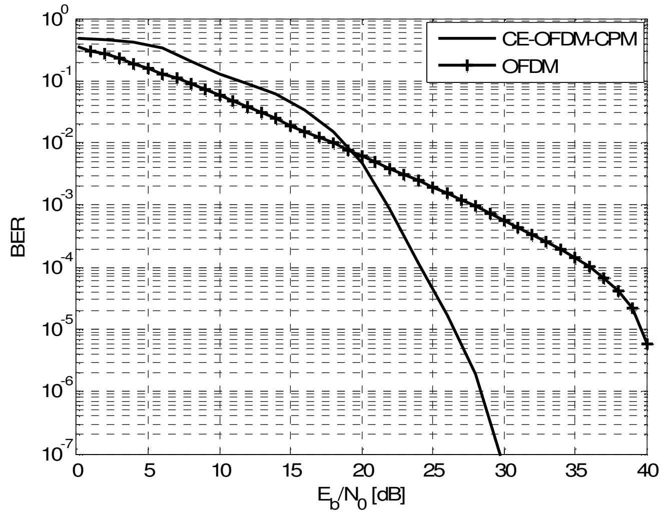

FIGURE 8: BER performances comparison of CE-OFDM, and OFDM systems under *HomePlug AV*

6. CONCLUSION

In this paper the performance of power line channel has been investigated. The propagation of high frequency signals in an indoor power network is strongly influenced by the connection of various electrical appliances, by the complexity and by the varying star topology of the power distribution installation. Therefore, a PLC application must be carefully designed and must be combined with proper experimentation, regarding signal transmission characteristics. Together with the PLC transmission environment, a possible modulation technique is introduced in order to create a complete picture of the PLC transmission. Design parameters for a CE-OFDM-CPM communication system for high rate data transmission over power lines are specified. OFDM-CPM is compared with conventional OFDM under HomePlug AV. CE-OFDM-CPM is shown to outperform OFDM at high E_b/N_0. However, at low E_b/N_0 the CE-OFDM-CPM phase demodulator receiver suffers from a threshold effect.

7. REFERENCES

1. Pavlidou N, Han Vinck A J, Yazdani J, Honary B. Power line communications: State of the art and future trends. IEEE Communications Magazine, 2003, 41(4): 34-40.

2. Gotz M, Rapp M, Dostert K. Power line channel characteristics and their effect on communication system design. IEEE Communications Magazine, 2004, 42(4): 78-86.

3. A. B. Gutierrez, A. Darmand, V. Watt, L. Ngalamou, “Design of an Analog Electronic Interface for a Power Line Based Telephony System”, IEEE-ISPLC 2006, Florida, USA, March 2006, pp. 232-238.

4. C. Papaleonidopoulos, C. G. Karagiannopoulos, D. P. Agoris, P. D. Bourkas, N. J. Theodorou. HF Signal Transmission over Power Lines and Transfer Function Measurement. Proc. of the Sixth IASTED International Conference. July 3-6, 2001, Rhodes, Greece. (502-505).

5. N. Sood, A. K Sharma, M. Uddin, “On Channel Estimation of OFDM-BPSK and –QPSK over Nakagami-m Fading Channels,” Signal Processing, An International Journal (SPIJ), Volume (4): Issue (4). 2010,pp. 239 – 246.

6. R. Prasad, OFDM for Wireless Communications Systems, Boston, MA, Artech House, 2004.

7. Ma Y H, So P L, Gunawan E. Performance analysis of OFDM systems for broadband power line communications under impulsive noise and multipath effects. IEEE Trans-actions on Power Delivery, 2005, 20(2): 674-682.

8. D. Wulich and L. Goldfeld, “Reduction of peak factor in orthogonal multicarrier modulation by amplitude limiting and coding,” IEEE Trans. Commununication, vol. 47, no. 1, pp. 18–21, January 1999.

9. L. Wang and C. Tellambura, “A simplified clipping and filtering techniques for PAR reduction in OFDM systems,” IEEE Signal Process. Lett., vol. 12, no. 6, pp. 453–456, June 2005.

10. W. Henkel and B. Wagner, “Another application for trellis shaping: PAR reduction for DMT (OFDM),” IEEE Trans. Commununication, vol. 48, no. 9, pp. 1471–1476, September 2000.

11. J. Sun Lee; H. Oh; J. Kim; J. Y. Kim;” Performance of scaled SLM for PAPR reduction of OFDM signal in PLC channels” Power Line Communications and Its Applications, IEEE International Symposium 2009,.

12. Y. Tsai and G. Zhang, “Orthogonal Frequency Division Multiplexingwith Phase Modulation and Constant Envelope Design,” in Proc. of IEEE Milcom 2005, Atlantic City, NJ, Oct. 2005.

13. S.C. Thompson, A.U. Ahmed, J.G. Proakis, and J.R. Zeidler, “Constant Envelope OFDM Phase Modulation: Spectral Containment, Signal Space Properties and Performance,” in Proc. of IEEE Milcom 2004, Monterey, CA, Nov. 2004.

14. S.C. Thompson, J.G. Proakis, and J.R. Zeidler, “Binary OFDM Phase Modulation,” in Proc. Of IEEE Milcom 2003, Boston, MA, Oct. 2003.

15. K. Dostert, Powerline communications, Prentice-Hall, 2001.

16. C. Tellambura, “Computation of the continuous-time PAR of an OFDM signal with BPSK subcarriers” IEEE Commun. Lett., vol. 5, pp.185–187,May2001.

17. Tor Aulin John B. ANderson and Carl-Erik Sundberg, Digital Phase Modu-

18. lation, Kluwer Academic Publishers, 1986;

19. T. Aulin, N. Rydbeck, and C. Sundberg, “Continuous phase modulation- Part I and II,” IEEE Trans. on Comm., vol. 29, no. 3, pp. 196–225, 1981.

20. S. C. Thompson, “Generating Real-Valued OFDM Signals with the Discrete Fourier Transform.” [Online]. Available: http://zeidler.ucsd.edu/~sct/pubs/t5.pdf.

21. S. C. Thompson, A. U. Ahmed, J. G. Proakis, and J. R. Zeidler, “Constant Envelope OFDM—Part II: Spectral Properties,” IEEE Trans. Commun., 2006.

22. J. G. Proakis and M. Salehi, communication systems Energineering. New Jersey: Prentice Hall, 1994.

23. H. Roberts, Angle Modulation. London: Peter Peregrinus Ltd., 1977.

24. “Spectral Estimation of Digital Signaling Using The Welch Method”. [Online]. Available: http://zeidler.ucsd.edu/~sct/holdings/welch/

25. C. K. Lin, S.C. Yeh, and H. H. Chen, “Bandwidth estimation of in-home power line networks,” in Proceedings of the 2007 IEEE International Symposium on Power line Communications and Its Applications, Pisa, Italy, Mar. 2007,pp.413–418.